Amplified Spontaneous Emission in Phenylethylammonium Methylammonium Lead Iodide Quasi-2D Perovskites

Supporting Information

*Matthew R. Leyden [1,2], Toshinori Matsushima [1,2,3], Chuanjiang Qin [1,2], Shibin Ruan [1,2], Hao Ye [1,2], Chihaya Adachi [1,2,3]**

[1] Center for Organic Photonics and Electronics Research (OPERA), Kyushu University, 744 Motooka, Nishi, Fukuoka 819-0395, Japan

[2] Japan Science and Technology Agency (JST), ERATO, Adachi Molecular Exciton Engineering Project, 744 Motooka, Nishi, Fukuoka 819-0395, Japan

[3] International Institute for Carbon Neutral Energy Research (WPI-I2CNER), Kyushu University, 744 Motooka, Nishi, Fukuoka 819-0395, Japan

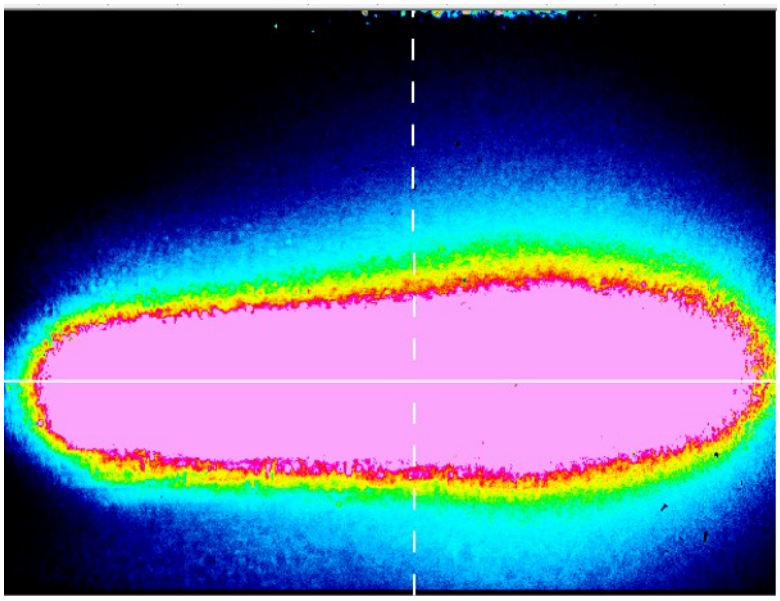

Figure S1. Excitation spot size measurement. The area of the spot size was measured using a CCD camera placed in the same plane as the sample. The area was assumed to be a rectangle with the area defined by 50% intensity measured by the CCD (5.87 x 1.69 m, ~0.01cm^2). The Image of spot size was measured at ~2 μJ/cm^2, which is lower than the values used for measurements to avoid over-saturating the camera and overestimating area.

Order (n)	PEAI (mg/ml)	MAI (mg/ml)	PbI_2 (mg/ml)
12	16.6	70.0	184
16	12.5	71.6	184
20	10.0	72.5	184
24	8.3	73.1	184
28	7.1	73.6	184
32	6.2	73.9	184
64	3.1	75.1	184
3D	0.0	76.3	184

Table S1. Concentrations of perovskite precursor solutions at 0.4 M.

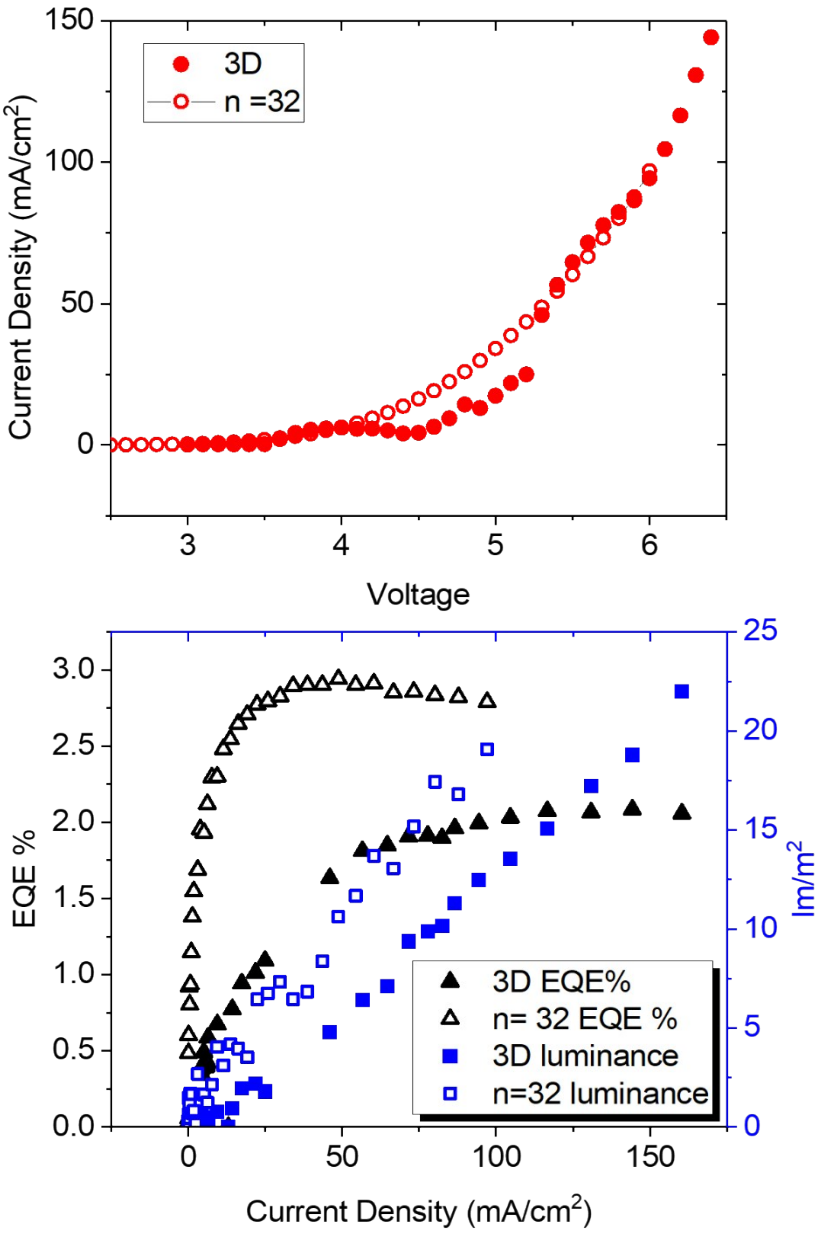

Figure S2. Example perovskite light emitting diodes. Light emitting diodes were prepared using the same protocol reported elsewhere.[1] Quasi 2D films have higher EQE values, are more stable, but will also begin to roll off at lower current densities. The Current/Luminance/EQE characteristics of the LED were measured simultaneously using an absolute EQE measurement system (C9920-12, Hamamatsu Photonics) connected to source meter (2400, Keithley) and multichannel analyzer (PMA-12, Hamamatsu Photonics).

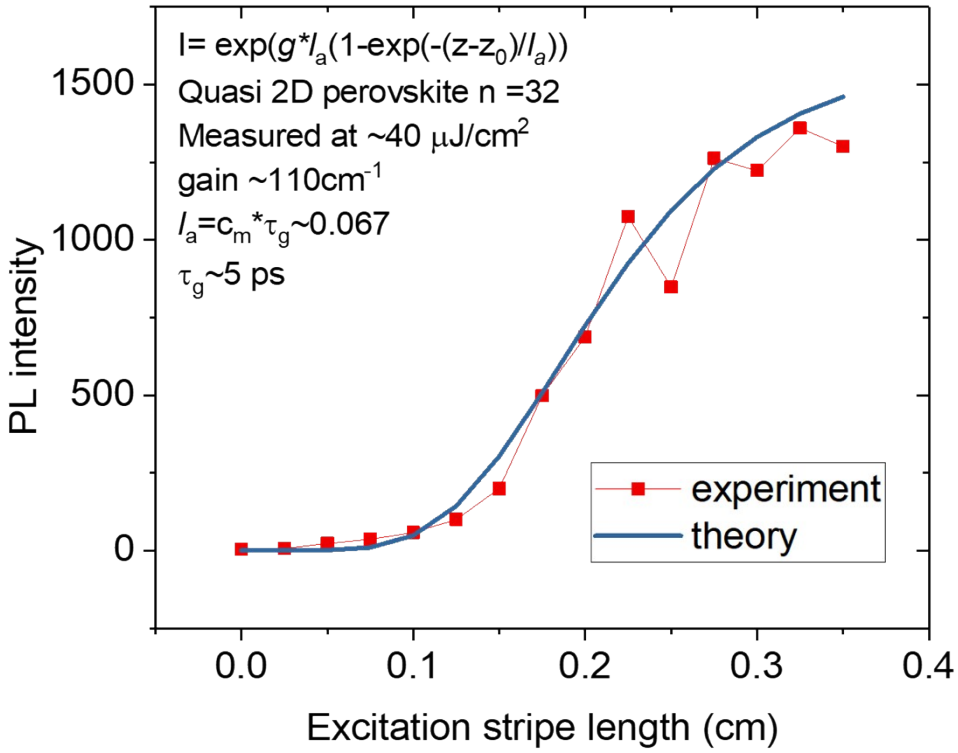

Figure S3. Variable stipe length measurement for determination of gain and gain lifetime in an example quasi 2D film (n=32). The gain and lifetime values shown are reasonably consistent with expectations.[2] The gain (g) and gain lifetime (τ_g) can be estimated from this fit. The speed of light within the medium (c_m) was estimated based on an index of refraction of ~2.3 measured by ellipsometry (Table S2).

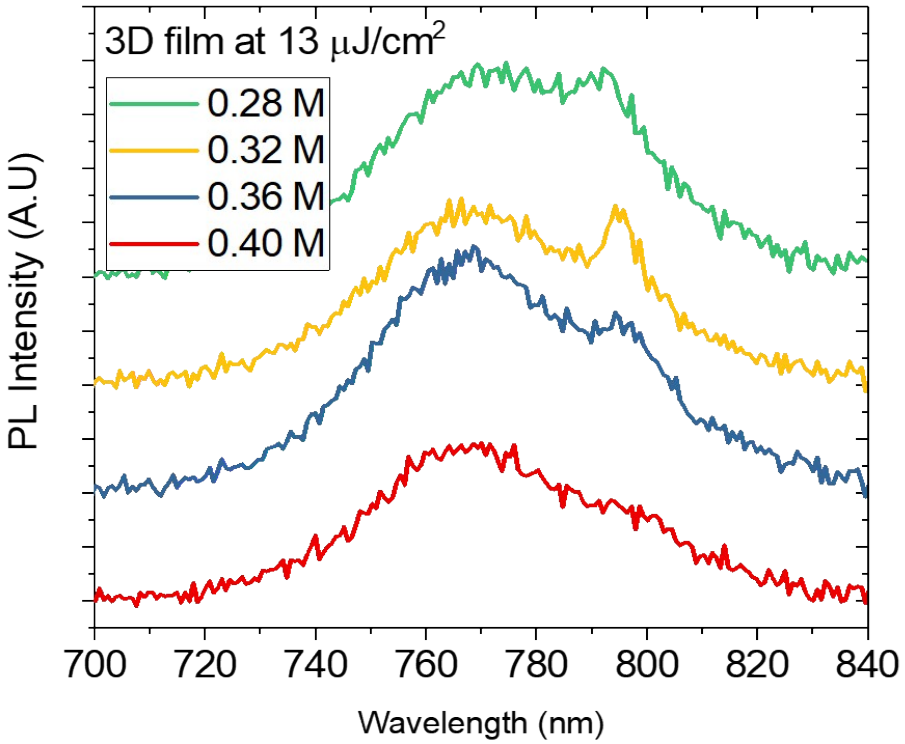

Figure S4. This figure shows that further reduction of the ASE threshold is possible by reducing the thickness of the film. The lowest threshold was observed around concentrations of ~0.32 M. A solution of 3D perovskite was prepared at 0.4 M concentration and then diluted to 0.36, 0.32, and 0.28 M.

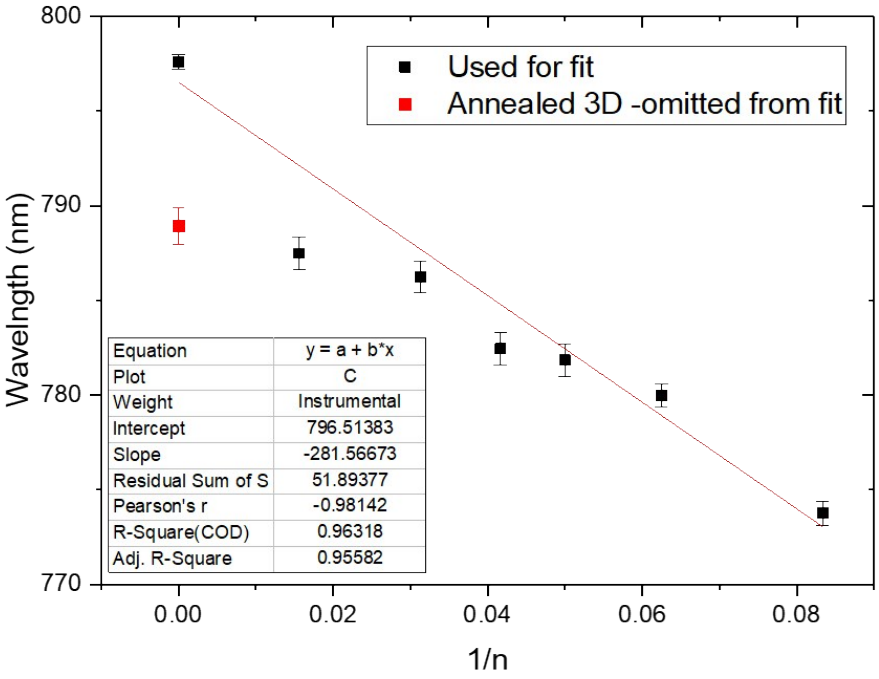

Figure S5. ASE peak location and inverse quasi 2D perovskite order (1/n). Here the peak location for the un-annealed film was used for the 3D perovskite to deconvolute from the impact of surface states. We can see that at low concentrations of PEA (n=64) the peak location was impacted by surface states and films were likely not protected by PEA passivation.

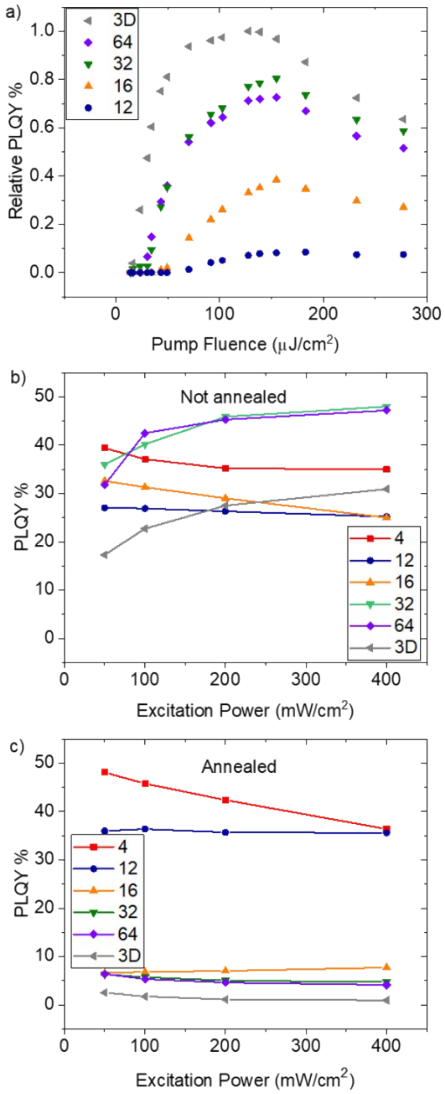

Figure S6. High order perovskite films showed less roll off in photoluminescent quantum yield, but are sensitive to annealing. a) Data from Fig. 2b is presented in terms of relative PLQY. The integrated peak area is divided by the pump fluence and normalized to the highest value. When presented in this way there is apparent roll off above 150 μJ/cm^2 b) Steady-state PLQY of un-annealed films. Films that increased in PLQY with excitation power had more intense ASE. c) Steady-state PLQY of annealed films. Annealing appeared to introduce trap states that significantly hampered steady state PLQY of higher order films. These are possibly the same surface states that blue shifted the emission in Fig. 3b. Lower order films appeared to be well passivated and increased in PLQY after annealing. Passivation of surface traps does not significantly impact ASE threshold.

Photoluminescence Quantum Yield (PLQY) Measurement. Continuous excitation from a 365 nm continuous UV-LED was irradiated normal to the perovskite films. These films were encapsulated with glass and UV resin, rather than covering with a film of PMMA. PL was detected by a multichannel photodetector (PMA-12, Hamamatsu) at an angle of 45 degrees. PLQY values were estimated by comparison of absorption and PL spectra of perovskite films with those of a vacuum-deposited tris(8-hydroxyquinolinato) aluminium (Alq3) film having a PLQY of 20%. Because the intensity of the light was measured at a fixed angle rather than collecting all light with an integrating sphere we acknowledge there is likely some error in the absolute magnitude of the PLQY measured. The data presented represents relative values and a best estimate of the absolute value of PLQY.

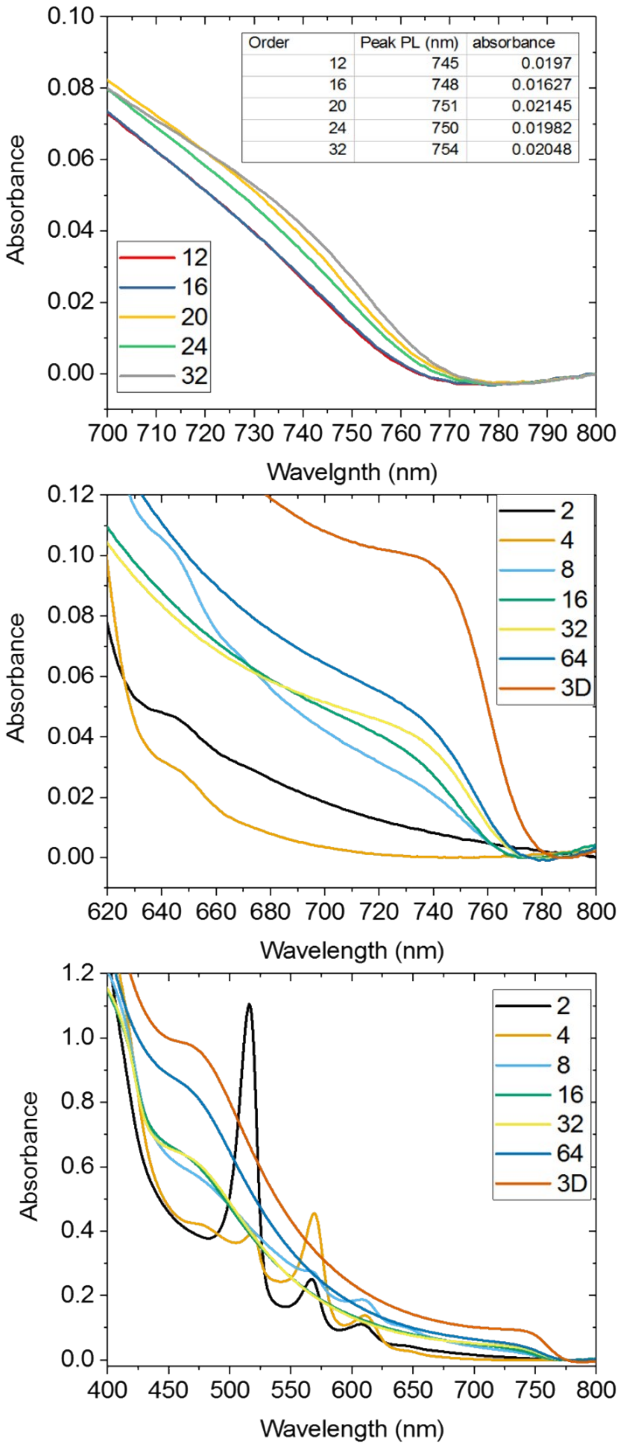

Figure S7. Absorption edge shifts along with PL peak for approximately constant levels of self-absorption. Absorption spectra of films were measured using a Lambda 950-PKA spectrophotometer (Perkin-Elmer).

Modeling of Dimensionality Distribution of Quasi 2D Perovskites

The concentration of PEAI determined the assumed order *n* of the film. We assumed that this film contained a proportion *P* of dimensionalities approximated by a Poisson distribution. A Poisson distribution was chosen as opposed to a Gaussian, as Gaussian will provide an unphysical distribution at lower orders.[3] Here *k* is the single dimensional contribution of a film of order n.

$$P(k,n) = (n^k \, e^{-n})/k!$$

We can assume that without charge transfer a grain of order n will behave like a single crystal of that order. Fortunately, a recent report measured the optical properties of analogous single crystals using n-butylammonium (n=1, 2, 3, 4, 5).[4] The largest crystal (n=5) had an optical bandgap of 1.85 eV, with a PL peak at ~ 670 nm. For example, if this crystal were a small component of a solution cast film of order 12 with an ASE peak ~770nm, the PL from crystals from orders 5 and lower would not be able to contribute to ASE. The PL contribution was assumed to be Gaussian in shape with 2σ values of 0.08 eV, or approximately the value of a single crystal. The values for the PL peak location E_n are taken from measured single crystal values up to order 5. Remaining orders are assumed to follow a 1/n relationship to the bulk value of 1.62 eV.

$$G(E,n) = \frac{1}{\sqrt{2\pi}} e^{\frac{-1}{2}\left(\frac{E-E_n}{\sigma}\right)^2}$$

The *ASE* peak energy location is taken from the experimental fit in Fig. S2b.

$$Threshold(n) \propto \sum_k \frac{1}{G(ASE,n)P(k,n)}$$

This sum is used to generate Fig S7a, where we see a monotonous increase in threshold over the range of orders presented in this work, but not as pronounced as experimental values (Fig 2c). A distribution of dimensionalities without charge transfer should have a higher threshold than a single dimensional film. Figs. S7 b and c show that lower order solution cast films would have a broader PL distribution than a high order film. Lower order films therefore have a more significant fraction of their PL that does not contribute to ASE. This distribution model cannot explain why low order films of a single dimensionality, such as 2D films, do not demonstrate ASE. Therefore there is likely an additional factor increasing the ASE threshold of PEAI containing films.

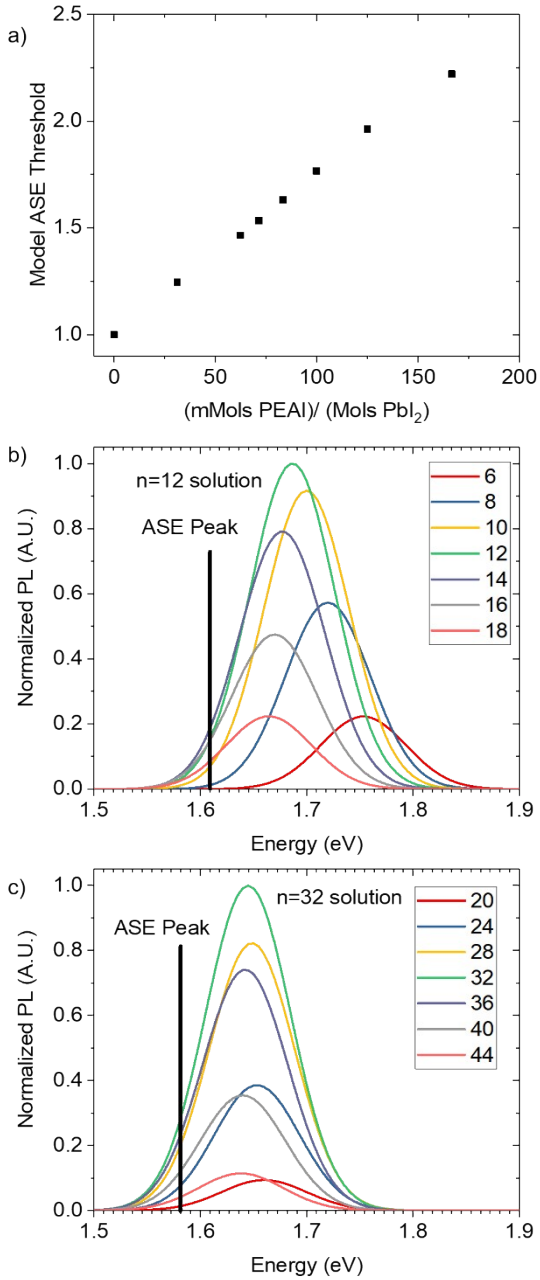

Figure S8. Modeling of dimensionalities within a quasi 2D film of average order n. a) Predicted ASE threshold of a quasi 2D film assuming a Poisson distribution of dimensionalities. b) Example predicted constituents of a film of order 12, along with the experimentally observed ASE peak location. There are significant components of the film that will not contribute to ASE. c) Example predicted constituents of a film of order 32, along with the experimentally observed ASE peak location. The higher order film has a narrower distribution of PL, and consequently a lower predicted threshold.

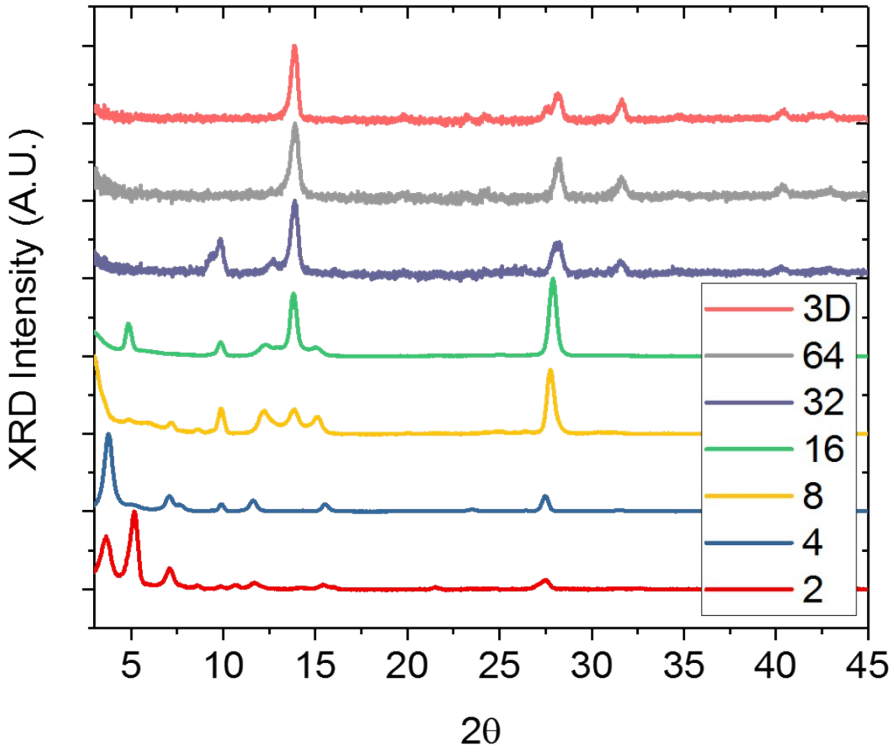

Figure S9. X-ray diffraction spectra of films at different order annealed for 5 min at 70 °C. The peak at around 2θ =10 is believed to be a DMF–perovskite complex. This is occasionally present due to the relatively short annealing time at low temperature.

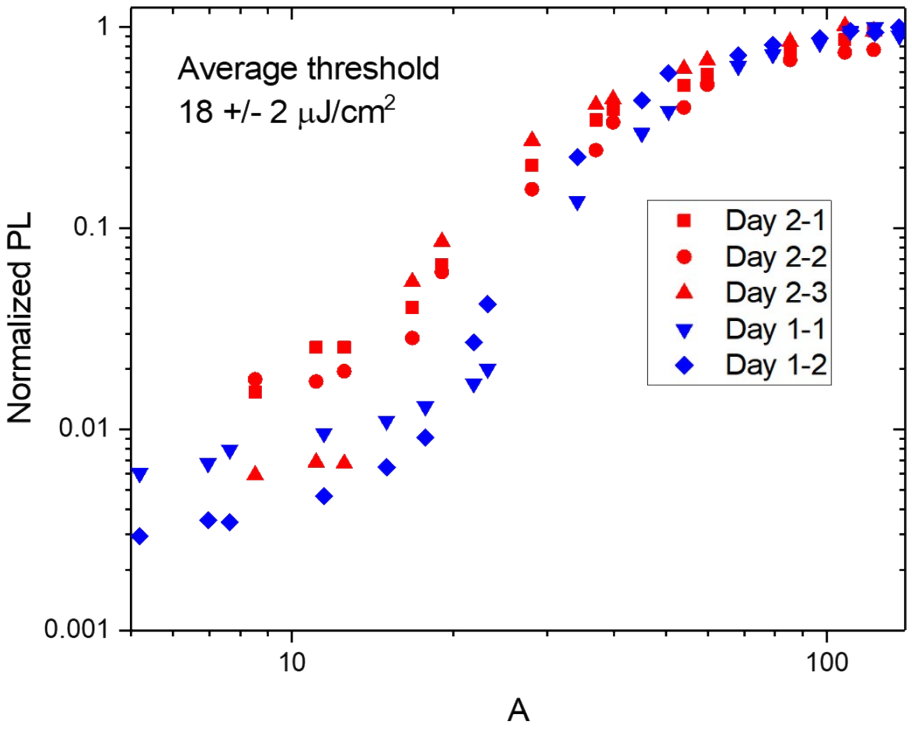

Figure S10. Estimation of error in threshold measurements. Shown above is a comparison of quasi 2D perovskite films of order 24 prepared at concentrations of 0.32 M. Films prepared and measured on the first day had thresholds 18, and 22 μJ/cm^2. On the second day, new films were prepared using the same stock of solution. The measurement system was realigned and spot size measured again. These films were measured to have thresholds of 16, 17 and 18 μJ/cm^2, but had lower gain than films from the first day. The average value of the threshold for this film was 18+/- 2 μJ/cm^2. Most variations seem to come from day to day changes in preparation and measurement conditions. Comparisons and best are made when films are prepared and measured all at the same time as done in figure 3.

		Index n	
wavelength (nm)	Order 12	Order 32	3D
850	2.25	2.30	2.30
900	2.23	2.27	2.28
950	2.21	2.25	2.25
1000	2.20	2.24	2.24

Table S2. Measurement of index of refraction by ellipsometry. Films were prepared using solutions at concentrations of 0.4M on silicon substrates. The perovskite film was assumed to be a Cauchy transparent material, so estimates of the index of refraction are limited to wavelengths above the absorption edge. Values at the emission wavelengths will likely be slightly higher than those presented here. Films including PEA had a slightly lower index at a given wavelength. We would like to thank Masayuki Yokoyama for assistance in ellipsometry measurements.

REFERENCES

(1) Xiao, Z.; Kerner, R. A.; Zhao, L.; Tran, N. L.; Lee, K. M.; Koh, T.-W.; Scholes, G. D.; Rand, B. P. Efficient Perovskite Light-Emitting Diodes Featuring Nanometre-Sized Crystallites. *Nat. Photonics* **2017**, *11* (2), 108.

(2) Xing, G.; Mathews, N.; Lim, S. S.; Yantara, N.; Liu, X.; Sabba, D.; Grätzel, M.; Mhaisalkar, S.; Sum, T. C. Low-Temperature Solution-Processed Wavelength-Tunable Perovskites for Lasing. *Nat. Mater.* **2014**, *13* (5), 476.

(3) Tuoriniemi, J.; Cornelis, G.; Hassellöv, M. Size Discrimination and Detection Capabilities of Single-Particle ICPMS for Environmental Analysis of Silver Nanoparticles. *Anal. Chem.* **2012**, *84* (9), 3965–3972.

(4) Blancon, J.-C.; Tsai, H.; Nie, W.; Stoumpos, C. C.; Pedesseau, L.; Katan, C.; Kepenekian, M.; Soe, C. M. M.; Appavoo, K.; Sfeir, M. Y.; et al. Extremely Efficient Internal Exciton Dissociation through Edge States in Layered 2D Perovskites. *Science* **2017**, eaal4211.